Biochimica et Biophysica Acta 1788 (2009) 1126–1137

Contents lists available at ScienceDirect

Biochimica et Biophysica Acta

journal homepage: www.elsevier.com/locate/bbamem

Hydrocarbon chains dominate coupling and phase coexistence in bilayers of natural phosphatidylcholines and sphingomyelins

Peter J. Quinn [a,*], Claude Wolf [b]

[a] Department of Biochemistry, King's College London, 150 Stamford Street, London SE1 9NN, UK
[b] Universite Pierre et Marie Curie-Paris6, UMRS538, CdR Saint Antoine, Faculte de Medecine, Paris 75012, France

ARTICLE INFO

Article history:
Received 21 October 2008
Received in revised form 2 December 2008
Accepted 17 December 2008
Available online 29 December 2008

Keywords:
Phospholipid
Sphingomyelin
Phosphatidylcholine
Membrane
Fluid phase
Bilayer phase immiscibility
X-ray diffraction

ABSTRACT

The structure and thermotropic phase behaviour of aqueous dispersions of egg phosphatidylcholine, egg sphingomyelin, bovine brain sphingomyelin and binary mixtures of phosphatidylcholine and sphingomyelins have been examined by synchrotron X-ray diffraction methods. Small-angle lamellar Bragg peaks and wide-angle X-ray scattering bands have been subjected to peak fitting procedures to identify coexisting gel and fluid as well as fluid–fluid bilayer structures. Molecular species of egg phosphatidylcholine exhibit fluid–fluid immiscibility throughout heating scans from 20 ° to 50 °C. Egg and brain sphingomyelins exhibit gel–fluid bilayer coexistence at temperatures below the main phase transition temperature and fluid–fluid phase coexistence at higher temperatures. Binary mixtures of equimolar proportions of egg phosphatidylcholine and either of the sphingomyelins show gel–fluid phase coexistence at temperatures below the gel phase transition temperature of the respective sphingomyelin. Binary mixtures containing egg sphingomyelin show fluid–fluid immiscibility at all temperatures of the heating scans whereas the fluid phase of mixtures comprising brain sphingomyelin are apparently miscible at all temperatures. An analysis of binary mixtures containing egg sphingomyelin and egg phosphatidylcholine in molar ratios 50:50, 67:33 and 83:17 at 50 °C to identify the composition of the lamellar phases indicated that the two phospholipids are immiscible in bilayers in the fluid phase. The results are discussed in terms of the role of intermolecular hydrogen bonds and hydrocarbon chain composition of sphingomyelins in maintaining coupling across fluid bilayers.

1. Introduction

The reason why the phospholipids of biological membranes are represented by such a wide range of molecular species is an enduring source of speculation in cell biology. These differ in hydrocarbon chain length, extent of unsaturation, mode and position of attachment to the molecular backbone. Equally intriguing are the biophysical processes that sense the stability of the lipid bilayer and the associated biochemical mechanisms in place to create and maintain the molecular species composition of each morphologically-distinct membrane within relatively narrow limits. These questions remain unanswered largely because methods have not yet been applied to unravel the details of structures of such complexity.

An understanding of the molecular mechanisms of membrane functions relies on knowledge of the principles governing the phase behaviour and stability of the membrane lipid bilayer matrix. In this connection the formation of lipid domain structures in biological membranes has excited considerable interest as a possible mechanism of control and modulation of a variety of physiological functions including trans-membrane signal transduction, membrane differentiation, fusion, apoptosis etc. [1–4]. Model membranes composed of lipid mixtures dispersed in aqueous media which exhibit phase separation and domain structures have been favoured systems to investigate the principles governing such behaviour. Amongst the multitude of lipid molecular species that dominate the outer leaflet of the plasma membrane of eukaryotic cells most are associated with the choline-containing phospholipids, phosphatidylcholine and sphingomyelin.

Molecular species of sphingomyelin, defined by the amide-linked fatty acid, present in cell membranes tend to have long, more saturated hydrocarbon substituents compared with phosphatidylcholines where the fatty acyl residues are shorter and unsaturated, particularly at the *sn*-2 position of the glycerol. Mixtures with extensive hydrocarbon chain inequivalence have been reported in some tissues such as eye lens lipids [5] and *N*-linked fatty acids exceeding C-26 appear integral to maintenance of the permeability barrier properties of skin [6]. There is evidence that the presence of cholesterol in asymmetric sphingolipid bilayers prevents interdigitation of hydrocarbon chains along the bilayer mid-plane [7] but because the distribution of cholesterol is non-random in complex mixtures transient interdigitation cannot be excluded. Indeed the interdigitation of sphingomyelin in transbilayer coupling has been conjectural since early X-ray measurements

* Corresponding author. Tel.: +44 207 848 4408; fax: +44 207 848 4500.
E-mail address: p.quinn@kcl.ac.uk (P.J. Quinn).

0005-2736/$ – see front matter.
doi:10.1016/j.bbamem.2008.12.011

showed that incorporation of cholesterol reduces the extent of methylene chain interdigitation [8].

Mixtures of natural phosphatidycholines and sphingomyelins are known to form bilayers with domains of coexisting gel phase, comprised of high melting point sphingomyelins, and fluid phase formed by low melting point molecular species of phospholipids at temperatures below and up to those approaching physiological values. The phase separation is achieved by zone refining effects whereby the low melting point lipids are excluded from lipids forming gel phase, supported by van der Waals cohesive interactions in the hydrophobic region of the bilayer, and intermolecular hydrogen bonds between the sphingomyelin molecules. Ternary mixtures of saturated and unsaturated phosphatidycholines in the presence of cholesterol representing the archetypal membrane "raft" domain separation have been thoroughly characterised to reveal coexisting liquid-ordered and liquid-disordered phase [9] with cholesterol asymmetrically distributed between the two [10].

A number of X-ray diffraction and calorimetric studies of aqueous dispersions of mixtures of sphingomyelins and phosphatidylcholines have been reported. Binary mixtures of bovine brain-SM/egg-PC [11] and porcine brain-SM/palmitoyl-oleoyl-PC [12] in which the gel to liquid–crystal phase transition temperature (Tm) of the constituent phospholipids differ by 40 °–42 °C exhibit gel–fluid phase coexistence at temperatures lower than high melting point SM component but are found to be completely miscible at temperatures above Tm of the SM. Mixtures of pure synthetic phospholipids, C16:0-SM/dimyristoyl-PC [13] and C18:0-SM/dipalmitoyl-PC [14], which differ much less in Tm values (17 ° and 3 °C, respectively) are completely miscible in both gel and fluid phases irrespective of the molar proportions of the phospholipids.

The effect of N-acyl chain length of sphingomyelin on miscibility with dimyristoyl-PC has been reported [15]. It was found that C16:0-SM mixes ideally but C24:0-SM is immiscible with the diacyl phospholipid. The effect of relative hydrocarbon chain lengths of C16:0-SM and saturated diacyl-PC on interaction and miscibility of the phospholipids in the gel state has been examined systematically using differential scanning calorimetry [16,17]. It was found that di-13:0-PC up to di-16:0-PC tended to mix ideally with C16:0-SM in all proportions in the gel phase with the longer chain species deviating the most from ideality. The Tm of di-12:0-PC was sufficiently different from that of C16:0-SM so that gel phase separation was observed. Gel phase separations were also observed with asymmetric 14:0/13:0-PC and 14:0/18:0-PC but other mixed acyl-PCs with less asymmetry all tended to mix ideally in the gel phase.

The overall conclusion from these studies was that phosphatidylcholines with acyl chain composition most closely matched to that of sphingomyelin had the most favourable interactions with some notable exceptions. Equimolar mixtures of egg-SM and di-16:0-PC, for example, showed a single phase transition endotherm judging them to be completely miscible and FT-IR spectroscopy showing an unchanged *gauche*/all-*trans* ratio in the presence of SM at temperatures either above or below Tm [18]. The librational motion of the fatty acyl chains, however, was affected, although only above Tm. By contrast, ESR spectroscopic probe studies of binary mixtures of egg-SM and egg-PC indicated extensive regions of coexistence of SM-rich and SM-poor domains, respectively in the gel and fluid phase, at temperatures below 37 °C but that the two phospholipids mixed well at higher temperatures [19]. Studies of the interaction of egg-SM and di-18:1-PC at 45 °C by pulse field gradient-NMR spectroscopy has shown that the diacylphospholipid diffuses by a monoexponential process that is only slightly slower than seen in dispersions of the pure phospholipid [20]. This was attributed to the presence of gel phase domains of SM indispersed with the fluid phase.

Another aspect of the phase separation in phospholipid mixtures that is somewhat neglected is the fact that the domains of fluid and gel phase are coupled across the bilayer. This is evident from X-ray diffraction studies of multilamellar dispersions of mixed molecular species of phosphatidylcholines in which the only lamellar reflections are those of the two discrete gel and fluid phases, respectively [10]. What is not yet clear is how the gel and fluid domains are coupled across the bilayer.

In the present study synchrotron X-ray diffraction methods have been used to examine the thermotropic phase behaviour of bilayers formed from mixed molecular species of phosphatidylcholine and sphingomyelin from egg-yolk and sphingomyelin from bovine brain during heating scans from 20 ° to 50 °C. Studies are also reported of binary mixtures of phosphatidylcholine and sphingomyelins to identify gel and fluid phase coexistence in these complex mixtures. The characterisation of bilayer properties relies on a detailed analysis of Bragg reflections from multilamellar dispersions using peak fitting methods to detect coexisting structures differing either or both in lamellar d-spacing or hydrocarbon chain packing. The results lead to the conclusion that the hydrocarbon chain substituents of choline-containing phospholipids are responsible for coupling domains of phospholipids across the bilayer as well as governing the miscibility of molecular species within the lateral plane of the bilayer.

2. Materials and methods

2.1. Phospholipid samples

Egg-yolk sphingomyelin (eggSM) and egg-yolk phosphatidylcholine (eggPC) were purchased from Sigma (Sigma-Aldrich, St.Quentin-Fallavier, France). Bovine brain sphingomyelin (brainSM) was purchased from (Avanti Polar Lipids, Alabaster, AL). A complete lipid analysis of each phospholipid was performed by ESI-tandem MS and the complete analyses are presented in Appendix 1 of the supplementary material. The fatty acid composition of the phospholipids was also examined by gas chromatography/mass spectrometry to confirm the absence of fatty acid degradation after exposure to the synchrotron X-ray beam. EggPC is comprised predominantly of 1-palmitoyl-2-oleoyl-*sn*-phosphocholine with lesser amounts of 1-stearoyl and 2-linoleoyl molecular species. EggSM is mostly amidified with palmitic acid and there are relatively smaller amounts of stearic and very long-chain fatty acids (C22:0, C24:0 and C24:1). BrainSM has a more complex molecular species composition than eggSM with a predominance of fatty acids amidified to sphingosine with hydrocarbon chain lengths C18:0, C20:0, C22:0 and C24 with some hydroxylated fatty acids.

2.2. Synchrotron X-ray diffraction measurements

Samples for X-ray diffraction examination were prepared by dissolving lipids in chloroform/methanol (2:1, vol/vol) and mixing them in the desired proportions (denoted as molar ratios in binary mixtures). The organic solvent was subsequently evaporated under a stream of oxygen-free dry nitrogen at 45 °C and any remaining traces of solvent were removed by a storage under high vacuum for 2 days at 20 °C. The dry lipids were hydrated with an equal weight of water. This was sufficient to fully hydrate the lipids according to lyotropic studies of these mixtures [11]. The lipids were stirred thoroughly with a thin needle, sealed under argon, and annealed by 50 thermal cycles between 20 and 65 °C ensuring a complete mixing of phospholipids. The samples were stored under argon at a temperature not below 4 °C. X-ray diffraction examination was performed after a 5 h sample equilibration at 20 °C and after careful stirring before transfer into the measurement cell. In order to check for possible dehydration or demixing of the components various control measurements were undertaken such as checking for reversibility of phase behaviour during subsequent heating and cooling cycles.

X-ray diffraction measurements were mainly performed at station 16.1 of the Daresbury Synchrotron Radiation Source (Cheshire, UK)

while some experiments were conducted at Spring8 in Japan. The X-ray wavelength was 0.141 nm with a beam geometry of ~0.2×0.5 mm in a mica sandwich cell with a surface of 2×5 mm. Simultaneous small-angle (SAXS) and wide-angle X-ray scattering (WAXS) intensities were recorded so that a correlation could be established between the mesophase repeat spacings and the packing arrangement of acyl chains. The SAXS quadrant detector response for correcting the small-angle scattering intensity for channel response was obtained using a static radioactive iron source. The sample to detector distance was 1.5 or 2.5 m and calibration of d-spacings was performed using hydrated rat-tail collagen ($d=67.1$ nm). The shorter configuration gave four-orders of lamellar phases. The wide-angle X-ray scattering intensity profiles were measured with a curved INEL detector (Instrumentation Electronique, Artenay, France) that was calibrated using the diffraction peaks from high-density polyethylene [21]. The lipid dispersion (20 μl) was sandwiched between two thin mica windows 0.5 mm apart and the measurement cell was mounted on a programmable temperature stage (Linkam, Surrey, UK). The temperature was monitored by a thermocouple inserted directly into the lipid dispersion [Quad Service, Poissy, France]. The setup, calibration, and facilities available on Station 16.1 are described comprehensively in the website; http://www.srs.dl.ac.uk/ncd/station161. Data reduction and analysis were performed using the OTOKO software version for a Personal Computer kindly provided by M. H. J. Koch [22] or using OriginPro8 software (OriginLab Corp).

2.3. Analysis of X-ray diffraction data

The small angle X-ray scattering intensity profiles were analysed using standard procedures [23]. Polarization and geometric corrections for line-width smearing were assessed by checking the symmetry of diffraction peaks in the present camera configuration using a sample of silver behenate ($d=5.838$ nm). The orders of reflection could all be fitted by Gaussian + Lorentz symmetrical functions with fitting coefficients greater than $R^2=0.99$. Deconvolution is consistent with the sample to detector distance used [24].

Apart from instrumental factors the width and intensity of Bragg peaks reflected from smectic mesophases are influenced by the structural order within the phase. The sources of this disorder in multibilayer dispersions and their effects on Bragg peaks have been considered and the implications for calculation of electron density profiles normal to the bilayer plane discussed [25]. Disorder can arise in four ways in phospholipid dispersions. 1. Macroscopic disorder which occurs when vigorous methods of dispersion aimed to mix the lipids are used resulting in a diverse population of uni-, oligo- and multilamellar vesicles. 2. Thermal disorder within the structure as the molecules oscillate about a mean position within the individual bilayers [26]. Such disorder results in loss in peak amplitude of the lamellar reflections and a corresponding increase in diffuse background scattering but no change in peak shape. The shape and amplitude of the wide-angle peaks, however, are both altered by the packing arrangement and order of the hydrocarbon chains of the lipids [27]. 3. Disorder caused by undulation of the bilayers within stacked arrays. 4. Stacking disorder in which the position of each bilayer with respect to adjacent bilayers fluctuates to generate an array with quasi long-range order. Both 3 and 4 result in loss of scattering intensity as well as peak width and the effect on peak width due to bilayer undulation tends to be greater for lipids in the fluid liquid–crystal phase compared with bilayers in gel or crystal phases. In the present analysis of Bragg peaks from records of SAXS/WAXS intensity profiles it is assumed that peak asymmetries from sample dispersions originate from different albeit closely spaced structures and the areas obtained by deconvolution of symmetric diffraction peaks provides a reasonable estimate of the relative mass of lipid contributing to the respective scattering peaks. In addition to greater angular resolution observed from higher order reflections from bilayer structures confirmation that different structures contribute to asymmetric Bragg peaks can often be obtained by demonstrating different temperature dependencies of the deconvolved peaks.

The scattering intensity data from the first three orders of the Bragg reflections from the multilamellar liposomes were used to construct electron density profiles [28]. After correction of the raw data for detector channel response and subtraction of the background scattering from both water and the sample cell, each of the deconvoluted Bragg peaks were fitted by a Lorentzian + Gaussian (Voigt) distribution. Similar curve fitting procedures were used to analyse the WAXS intensity bands. The fittings were performed with the software package Peakfit 4.12 (Systat Software, Inc.). The square root of integrated peak intensity $I(h)$ is used to determine the form factor $F(h)$ of each respective reflection:

$$F(h) = h\sqrt{I(h)},$$

h = order of peak reflection, $I(h)$ = integrated intensity of each respective reflection.

The electron density profile is calculated by the Fourier synthesis:

$$\rho(z) = \sum \pm F(h)\cos(2\pi hz/d),$$

$d = d_{spacing} = d_{pp} + d_W$ (d_{pp}: phosphate–phosphate bilayer thickness, d_W: hydration layer) at a resolution of $d/2$ $h_{max}=1$ nm for 3 orders.

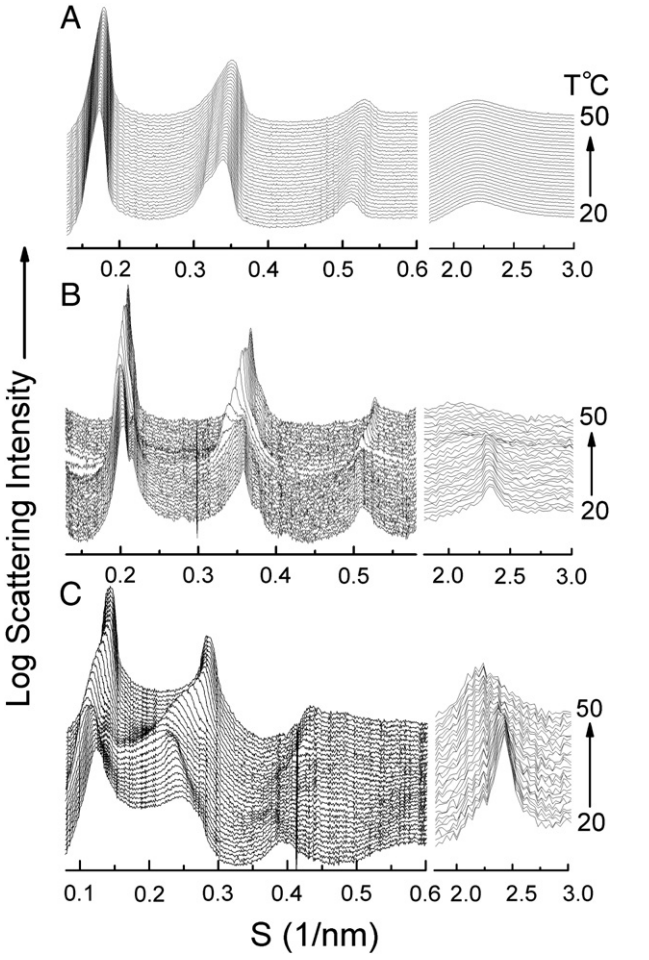

Fig. 1. SAXS/WAXS intensity profiles recorded from aqueous dispersions of (A) egg-yolk phosphatidylcholine; (B) egg-yolk sphingomyelin; (C) bovine-brain sphingomyelin. The samples were equilibrated at 20 °C before heating at 2 °C/min. to 50 °C. Scattering patterns were recorded at 30 s intervals.

The phase sign of each diffraction order is either positive or negative for a centro symmetric electron density profile for Lo and Ld phases. The phasing choice for the lamellar gel and liquid crystal phases (− − + −) were taken because uniquely this single combination of signs provides the expected electron density profile with the minimum density appropriately located at the bilayer centre, the maxima at the 2 electron rich interfaces and the hydration layer density (0.33e-/A^3) at the intermediate value on the relative electron density scale. All other phase combinations result in aberrant distributions.

3. Results

X-ray diffraction patterns from multilamellar dispersions of lipids obtained from extracts of biological tissues are complex and reflect the range of molecular species that are present. This complexity is shown in the SAXS/WAXS profiles recorded during temperature scans from 20 °C to 50 °C of three choline-containing phospholipids shown in Fig. 1. The scattering intensity is plotted on a logarithmic scale to emphasize the higher order reflections. EggPC (Fig. 1A) and sphingomyelins from egg (Fig. 1B) and bovine brain (Fig. 1C) all show Bragg reflections in the SAXS region in the order 1:2:3 consistent with lamellar phases over the temperature range of the scan. In the WAXS region eggPC shows a broad scattering band typical of liquid hydrocarbons whereas both sphingomyelins undergo gel to liquid–crystal phase transitions during the heating scans.

The X-ray scattering intensity profiles shown in Fig. 1 have been subjected to detailed analysis using peak fitting routines to identify the characteristics of coexisting phases. This is exemplified in Fig. 2

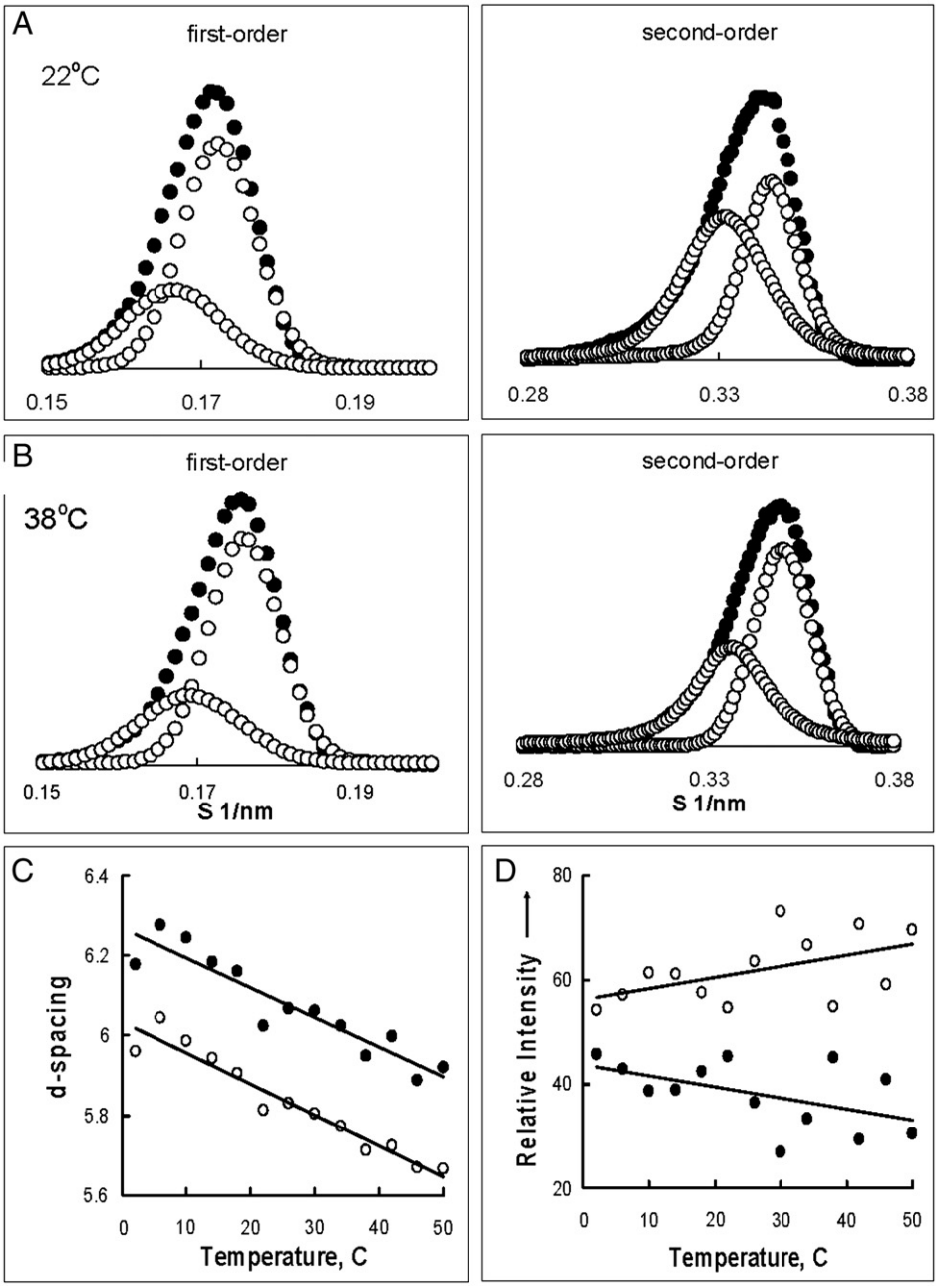

Fig. 2. Structural changes in egg phosphatidylcholine during an initial heating from 20 °C to 50 °C obtained from the data shown in Fig. 1A. The first and second-order Bragg reflections recorded at (A) 22 °C and (B) 38 °C (●) are deconvolved into two symmetric peaks (○) (statistical data for the fits are presented in the supplementary material). (C) Lamellar d-spacings and (D) relative X-ray scattering intensities of the two lamellar structures.

which shows the fits of two peaks to the first two orders of Bragg reflections from eggPC given in Fig. 1A at temperatures of 22 °C (Fig. 2A) and 38 °C (Fig. 2B). The protocol used to perform the peak fitting and statistical analyses of the results are presented in Appendix 2 of the supplementary material. The results obtained from the analysis of all three orders of the SAXS data in Fig. 1A are summarised in Fig. 2C and D. These figures show temperature-dependence of d-spacings and relative X-ray scattering intensity of the two deconvoluted peaks, respectively, throughout the heating scan. It can be seen that the lamellar d-spacing of both structures decrease in tandem with increasing temperature and at the same time the lamellar structure of greater d-spacing is transformed into the structure of smaller d-spacing. Clearly it is not possible to distinguish the two structures on the basis of the dependence of their respective lamellar repeat spacings on temperature.

To determine the way the transformation between the two coexisting bilayer structures takes place electron density distribution through the lamellar repeats were calculated. The results are presented in Fig. 3. The resolution that could be achieved with these calculations is relatively low because they are based on only three orders of reflection but the relative electron distributions between the different structures indicate a consistent trend. The lamellar structure of smaller d-spacing has thicker bilayers and thinner hydration layers at comparable temperatures than those of the lamellar structure of greater d-spacing. The decrease in d-spacing with increasing temperature was the result of a decrease in bilayer thickness of both structures rather than a change in dimensions of the respective water channels. This is consistent with a difference in molecular species composition between the two bilayer structures.

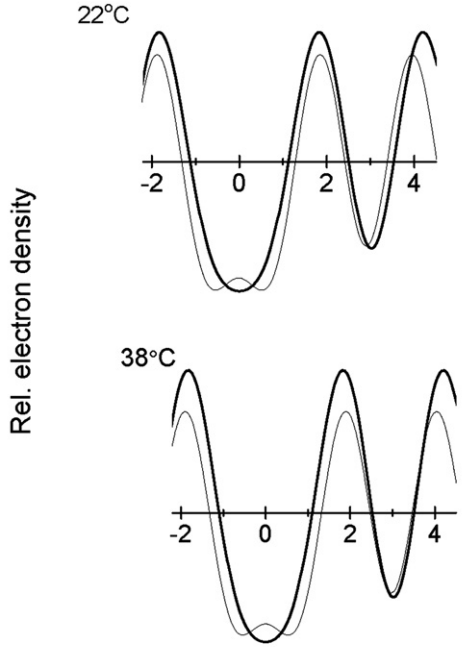

Peak	d (nm)	d_{pp} (nm)	d_w (nm)
Peak 1, 22°C	6.03	3.68	2.35
38°C	5.94	3.60	2.34
Peak 2, 22°C	5.81	3.72	2.09
38°C	5.70	3.64	2.05

Fig. 3. Relative electron density profiles through the lamellar repeat structures shown in Fig. 2A and B, respectively. Peak 1 is shown as thick lines and Peak 2 as fine lines. The table shows parameters of lamellar repeat, bilayer thickness and dimensions of the water layer for the two bilayers at each temperature.

Those factors that are responsible for the difference in structure favour the structure of smaller lamellar repeat spacing which has the thicker bilayers with thinner water layers as the temperature increases. Since these temperature-dependent changes in structure are reversible the possibility of differences in sample hydration can be discounted.

Sphingomyelins from egg and brain are comprised of more saturated hydrocarbons than phosphatidylcholines from these sources. One consequence of this is the gel to liquid–crystal phase transition temperatures of most molecular species of sphingomyelin occurs at or close to physiological temperatures. This is exemplified in the detailed analyses of the SAXS/WAXS intensity profiles of eggSM presented in Fig. 1B and shown in Fig. 4. The lamellar Bragg peaks at temperatures below 40 °C can be deconvolved into two coexisting bilayer structures which we assign to a bilayer gel phase of d-spacing about 6.25 nm and an interdigitated bilayer structure with a d-spacing of 5.7 nm at 20 °C. The assignment of the interdigitated gel phase is based on (a) the relative proportion of molecular species with *N*-acyl chains greater than C-18 vs the relative scattering intensity of the lamellar phase of shorter d-pacing (Fig. 4A and B) (b) the bilayer thickness of Peak 2 of only 3.36 nm (Fig. 4C) (c) the disappearance of a sharp peak at 0.42 nm at 40 °C (Fig. 4D) (d) a reappearance of the lamellar d-spacing only after relatively long equilibration periods at temperatures less than 40 °C [29]. The interdigitated gel phase that is present over the temperature range 30 ° to 40 °C is converted into the lamellar gel phase before transition to the liquid–crystal phase. The gel phase is characterised by a SAXS peak located at a d-spacing of 12.05 nm at 20 °C decreasing progressively to 11.85 nm before disappearing at a temperature coinciding with the disappearance of the lamellar d-spacing at 6.25 nm and is assigned to a ripple phase structure (data not shown). These assignments are not only consistent with the difference in d-spacing but also in the temperature dependencies of the two structures; the interdigitated phase shows no change in repeat spacing over the temperature range 20 ° to 38 °C. Transition from gel to liquid–crystal phase takes place in both structures at about 38–40 °C and is associated with a disappearance of the d-spacing associated with the interdigitated phase and a sharp decrease in lamellar d-spacing as the gel phase is transformed into the fluid phase. These changes are also seen in the relative X-ray scattering intensity of the different lamellar phases shown in Fig. 4B. The changes in bilayer structure of the two lamellar gel phases are seen from the differences in electron density distribution across the repeat structure shown if Fig. 4C. Thus the increase in d-spacing of the gel phase between 20 ° and 35 °C is largely due to an increase in the dimensions of the water layer. The thickness of the bilayers of the interdigitated phase decreases from 3.71 nm to 3.36 nm over this temperature range but the d-spacing is maintained at a constant value by a corresponding increase in water layer thickness. Fig. 4D summarises the analysis of the WAXS intensity data and shows that the sharp peak at 0.42 nm characteristic of gel phase dominates the scattering in the wide-angle region and shifts to a weaker scattering band upon heating above 40 °C. There is a close correlation between the SAXS and WAXS peaks in defining the gel to liquid–crystal phase transition of eggSM.

The analysis of SAXS/WAXS intensity patterns recorded from brainSM (Fig. 1C) shows a more complex behaviour than that of eggSM. This can be seen in Fig. 5. Two coexisting bilayer structures can be deconvolved from the Bragg peaks at all temperatures over the range of the heating scan. The lamellar structure of greater d-spacing (8 nm at 20 °C, Fig. 5A) is predominantly a gel phase with a wide-angle scattering maximum of 0.42 nm (Fig. 5D). Nevertheless there appears to be considerable disorder in packing of the hydrocarbon chains because about 30% of the total scattering intensity in the WAXS region at 20 °C arises from hydrocarbon in a disordered state. This phase is progressively transformed into a lamellar liquid–crystal phase the transformation of which is complete at a temperature of

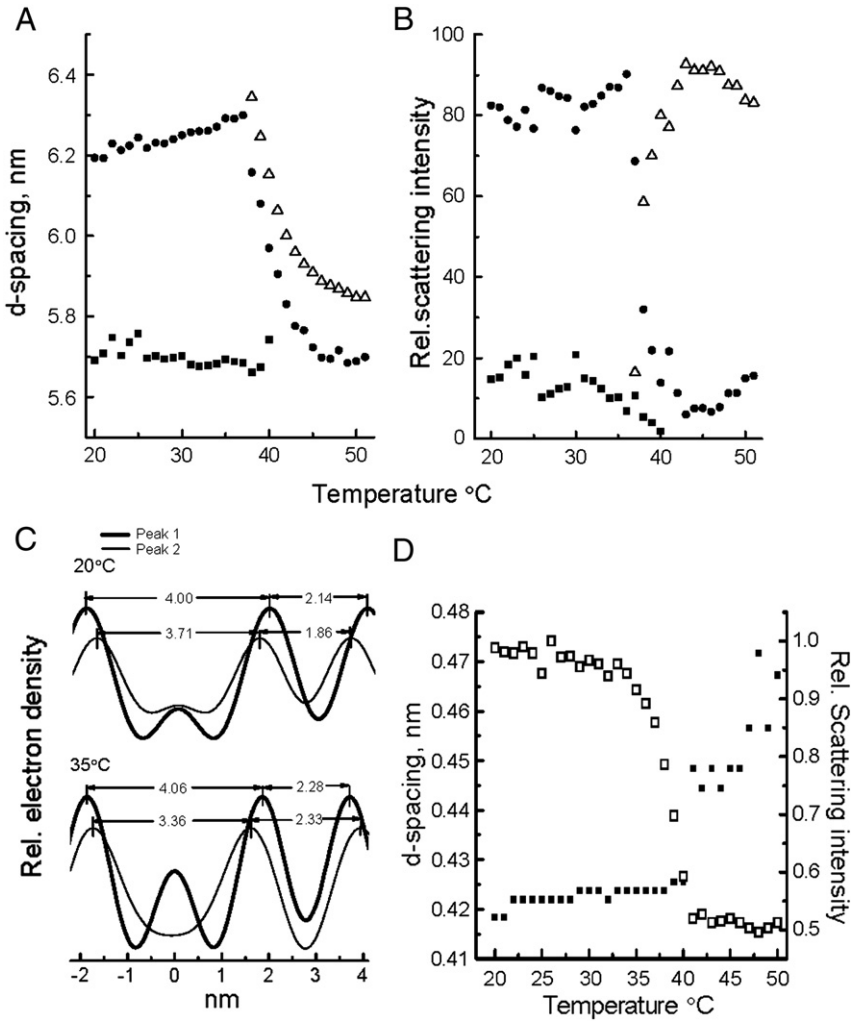

Fig. 4. Structural changes in egg sphingomyelin during an initial heating from 20 °C to 50 °C obtained from the data shown in Fig. 1B. Lamellar d-spacing (A) and relative X-ray scattering intensity (B) of two lamellar structures deconvolved from the Bragg peaks plotted as a function of temperature (the symbols in B correspond to the peaks in A). ■, represents the structure assigned as interdigitated lamellar gel phase. (C) Relative electron density profiles through the lamellar repeat structures at 20 °C and 35 °C. Peak 2 is designated as interdigitated lamellar gel phase. (D) d-spacing (■) and relative scattering intensity (□) of the WAXS intensity maximum plotted as a function of temperature.

33 °C. The increase in d-spacings and the changes in peak shape observed during heating from 20 ° to 33 °C are reminiscent of ripple structures but no Bragg peaks at higher d-spacings are detected. The Bragg peaks initially sharpen and then broaden towards the completion of the transition (Fig. 5C). The lamellar structure of smaller d-spacing, on the other hand, exhibits different thermotropic behaviour and arises from a different structure. This is also assigned as a gel phase at 20 °C and contributes about 15% of the total scattering intensity of the SAXS peaks. The structure remains relatively unchanged during heating up to about 39 °C whereupon it is transformed into another lamellar phase that appears to coexist with the dominant lamellar liquid–crystal phase. Because two lamellar phase transitions are detected, one at 33 °C and the other at 39 °C, the implication is that the molecular species represented in the two structures are different.

To investigate the phase behaviour of mixtures of eggPC with sphingomyelins SAXS/WAXS intensity profiles were recorded during heating scans from 20 ° to 50 °°C from mixtures containing equimolar proportions of the two phospholipid classes. The results obtained from the heating scan of eggPC and eggSM are presented in Fig. 6. An overview of the SAXS/WAXS intensity profiles showing Bragg peaks of the first two orders of the lamellar structures are seen in Fig. 6A. Deconvolution of the first-order Bragg reflection was best fitted by three peaks (Fig. 6B). The SAXS peak of greatest d-spacing is assigned to a lamellar gel phase of eggSM because this peak can no longer be detected at about 33 °C (Fig. 6C) which coincides with disappearance (Fig. 6E) of a WAXS peak deconvolved from the wide-angle scattering band centred at about 0.41 nm (Fig. 6D). The temperature-dependence of the lamellar d-spacing is opposite to that observed in the pure eggSM and may indicate that the phase separated gel phase does not form either a ripple structure or an interdigitated bilayer phase. Furthermore, less than half of the eggSM present in the mixture contributes to scattering attributed to the gel phase and the temperature of the gel to liquid–crystal phase transition is 7–8 °C lower than seen in the pure lipid. This suggests that the gel phase is perturbed by the presence of eggPC in the mixture. Judging from the changes in relative X-ray scattering intensities of the lamellar Bragg peaks of the two remaining fluid phases between about 28 °C and 35 °C (Fig. 6C) it may be concluded that the gel phase comprised of high melting point molecular species of eggSM are transformed into the fluid bilayer of greater d-spacing. The two fluid bilayer structures coexist over the entire range of the temperature scan achieving constant scattering intensities at all temperatures above the gel to liquid–crystal phase transition of the gel phase bilayers of sphingomyelin.

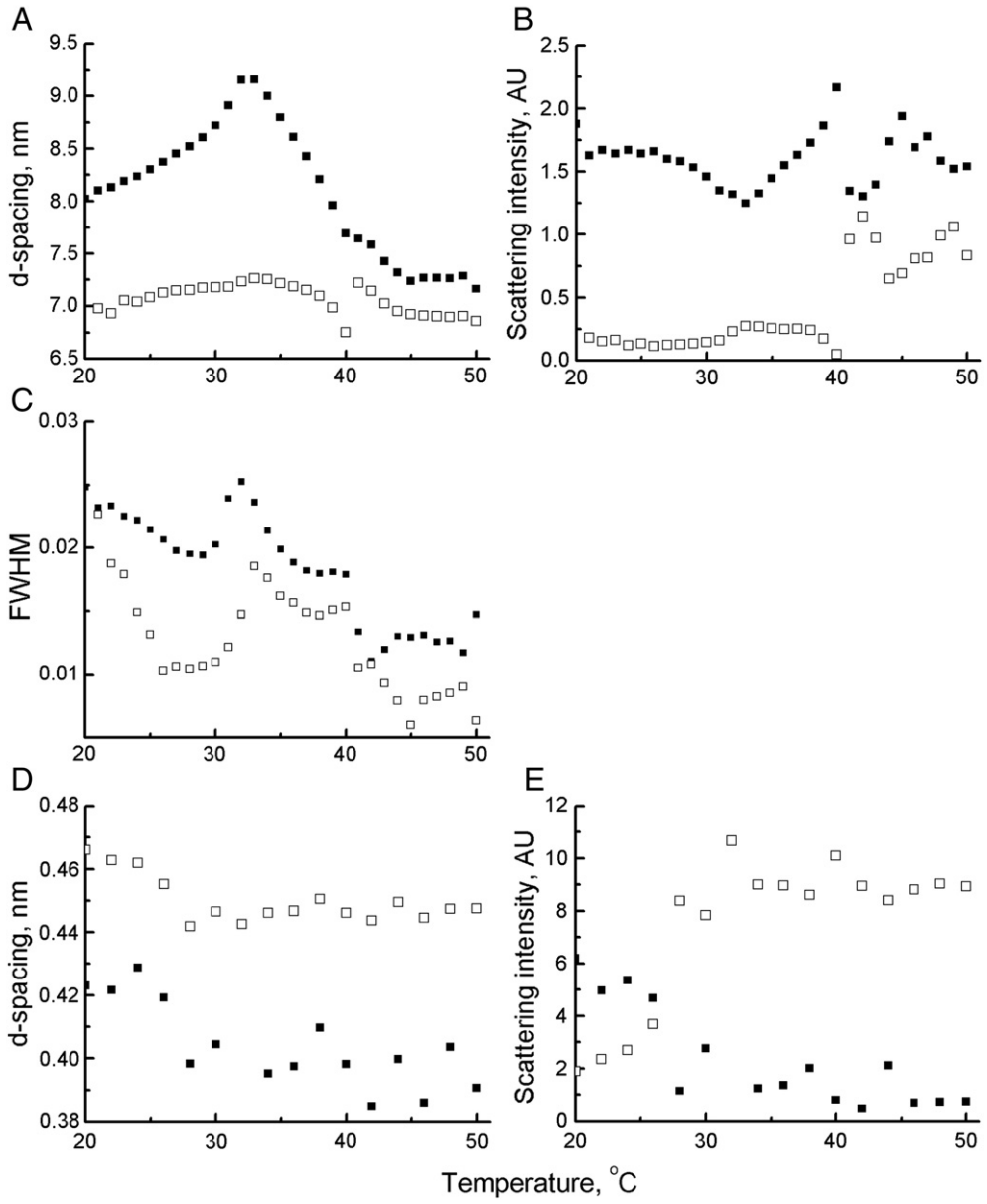

Fig. 5. Structural changes in bovine-brain sphingomyelin during an initial heating from 20 °C to 50 °C obtained from the data shown in Fig. 1C. Lamellar d-spacing (A) and relative X-ray scattering intensity (B) of two lamellar structures deconvolved from the Bragg peaks plotted as a function of temperature. (C) Full width at half maximum (FWHM) scattering intensity of the two first-order Bragg peaks from the lamellar structure. (D) d-spacing; (E) X-ray scattering intensity, respectively, of two peaks deconvolved from the WAXS region.

The features observed in the equimolar mixture of eggPC and brainSM appear to be more straightforward (Fig. 7). The Bragg peaks seen in the SAXS profiles are fitted reliably to a single lamellar repeat which exhibits biphasic behaviour with respect to d-spacing (Fig. 7B) and sharpness (Fig. 7C) during the heating scan. Thus the rate of decrease in lamellar d-spacing with increasing temperature is relatively steep up to a temperature of about 33 °C whereupon the rate of decrease is less during subsequent heating to 50 °C. The width of the peak also decreases up to 33 °C but broadens progressively at higher temperatures. The inflection point at 33 °C coincides with the onset of the transition of a coexisting gel phase evidenced from a relatively sharp peak (Fig. 7E) at a d-spacing of about 0.415 nm (Fig. 7D) deconvolved from the WAXS intensity band. As with the eggSM, the gel phase is comprised of the non-interdigitated high melting point molecular species of sphingomyelin. It is noteworthy that coexistence of the fluid and gel phases in this mixture is detected only in the WAXS region arising from the packing of the hydrocarbon chains; no coexisting lamellar structures can be deconvolved from the scattering in the small-angle region.

A comparison of the results obtained with equimolar mixtures of eggPC with eggSM (Fig. 6) and brainSM (Fig. 7) indicated that the former consisted of coexisting fluid bilayers whereas the components of the latter were miscible at temperatures above the Tm of brainSM. To further investigate fluid–fluid immiscibility aqueous dispersions of mixtures of eggSM and brainSM in molar proportions with eggPC of 50:50, 67:33 and 83:17 were examined at 50 °C, a temperature at which all phospholipids in the mixtures are in a liquid–crystal phase as seen from the peaks in the WAXS region. The first two orders of the SAXS intensity profiles, plotted on a logarithmic scale, from these mixtures are presented in Fig. 8. In the eggSM: eggPC mixtures (Fig. 8A) a peak corresponding to the d-spacing of eggSM can be deconvolved in all mixtures. The peak assigned to eggPC is shifted to

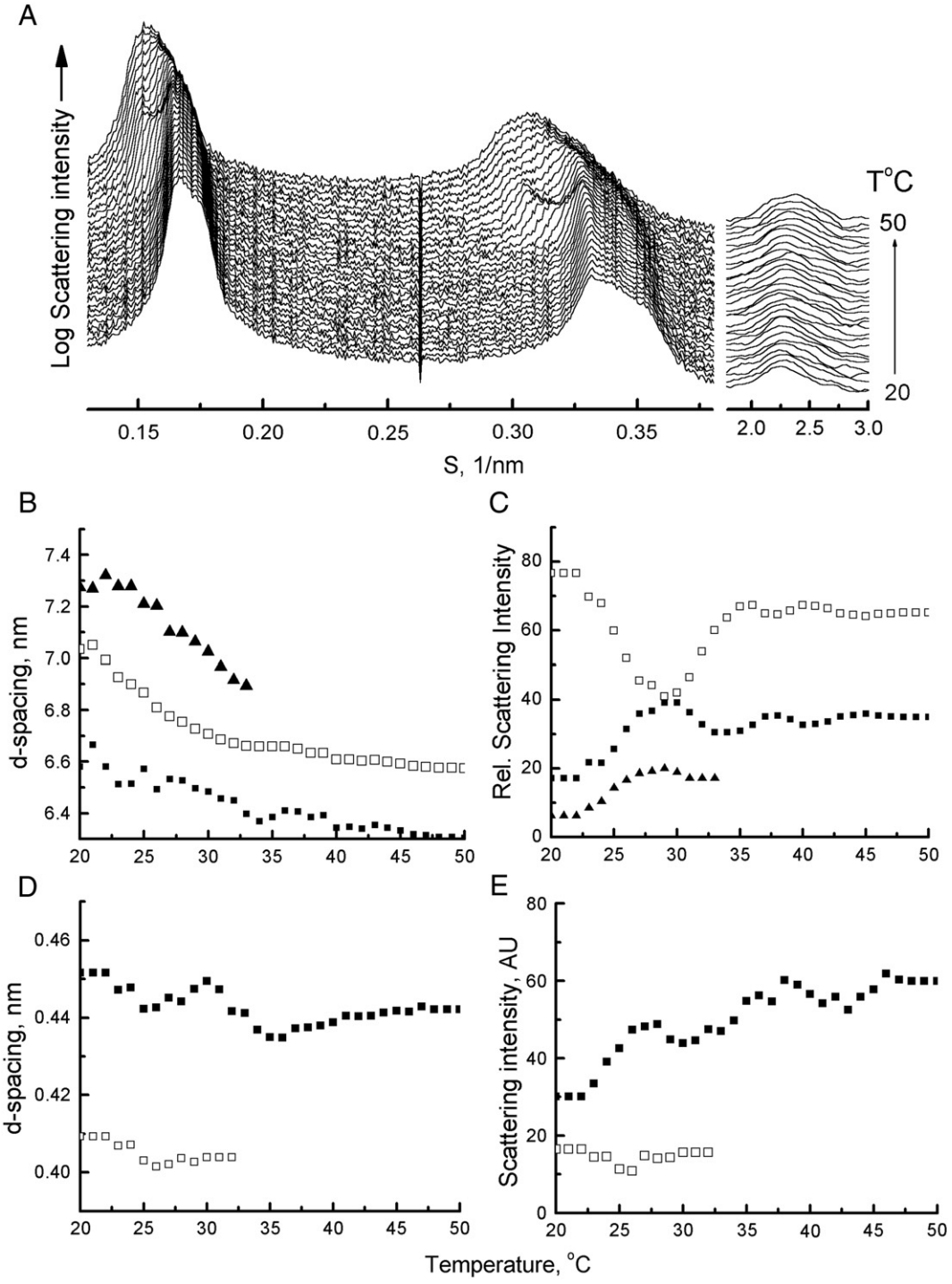

Fig. 6. (A) SAXS/WAXS intensity profiles recorded from an aqueous dispersion of an equimolar mixture of egg-yolk phosphatidylcholine and egg-yolk sphingomyelin during an initial heating scan from 20 °C to 50 °C at 2 °C/min. Scattering patterns were recorded at 30 s intervals. (B) Lamellar d-spacings and (C) relative X-ray scattering intensity of deconvolved first-order Bragg peaks shown in A. (D) WAXS d-spacings and E. scattering intensity of deconvolved peaks shown in A.

higher d-spacing. By contrast, brainSM does not retain an identifiable lamellar repeat spacing in mixtures with eggPC but the single broad peak adopts a d-spacing intermediate between pure brainSM and eggPC at a value dependent on the proportion of the two phospholipid components of the mixture.

Peak deconvolutions of the first three orders of reflection in the SAXS region of the eggSM: eggPC mixtures at 50 °C were performed and the results are presented in Table 1. Peak 1 is assigned to eggSM on the basis of the lamellar repeat spacing which in pure eggSM has a value of about 5.9 nm at 50 °C (Fig. 4A). The d-spacings of the two peaks were derived from the mean of peaks deconvolved from all orders of detectable Bragg reflections. Deconvolutions of the first and second-order Bragg peaks are shown in Appendix 3 of the supplementary material. EggSM has a similar d-spacing in all mixtures and the peak becomes sharper (>Int/FWHM) as the proportion of eggPC in the mixture decreases. The relative X-ray scattering intensity from eggSM increases as the proportion of eggPC in the mixture decreases. The d-spacing of Peak 2 increases with decreasing proportion of eggPC

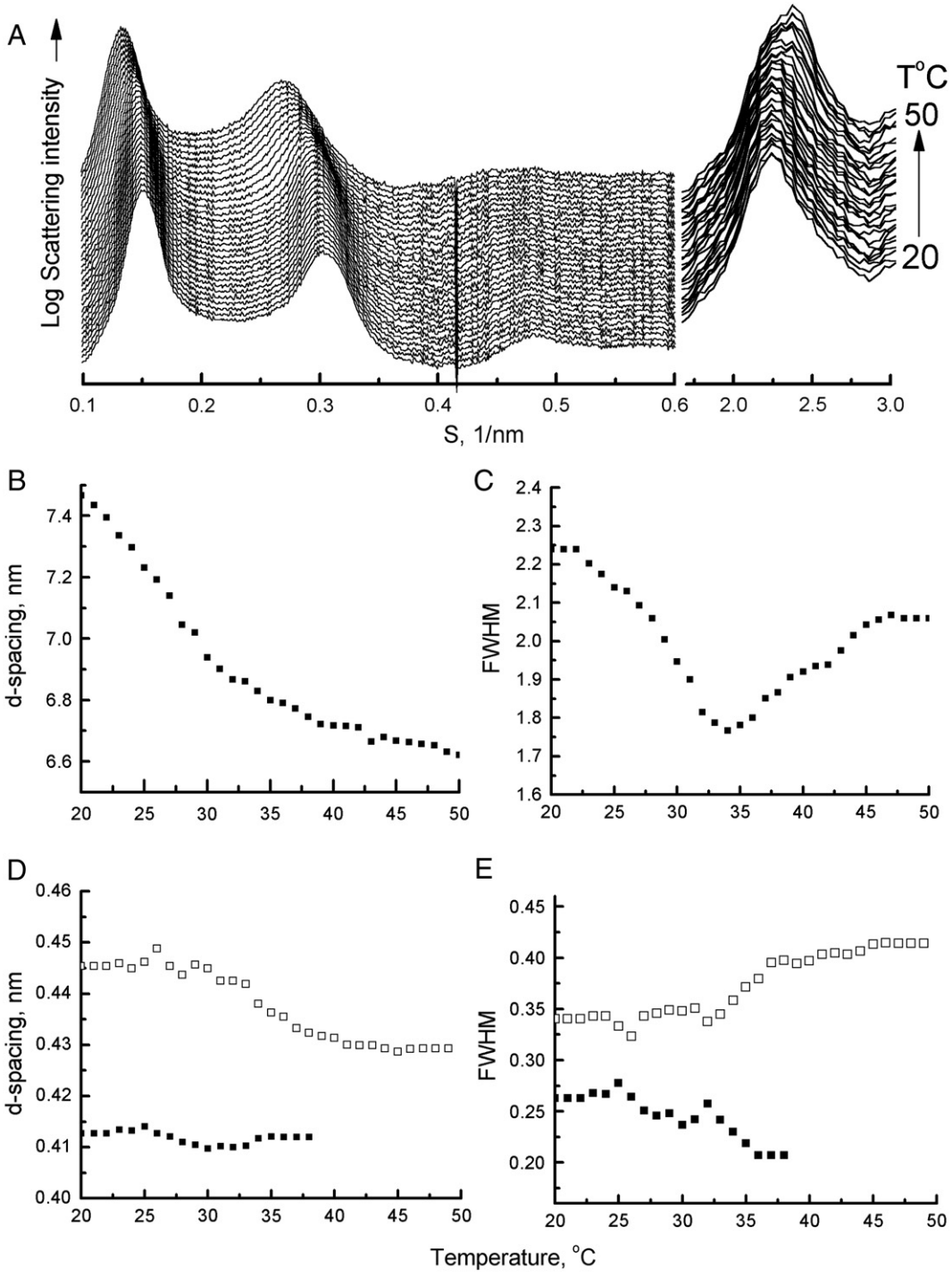

Fig. 7. (A) SAXS/WAXS intensity profiles recorded from an aqueous dispersion of an equimolar mixture of egg-yolk phosphatidylcholine and brain sphingomyelin during an initial heating scan from 20 °C to 50 °C at 2 °C/min. Scattering patterns were recorded at 30 s intervals. (B) Lamellar d-spacings and (C) Full width at half maximum of deconvolved first-order Bragg peaks shown in A. (D) WAXS d-spacings and (E) full width at half maximum of two peaks deconvolved from the wide-angle scattering band shown in A.

in the mixture and is progressively broadened. By contrast, the peak assigned to eggSM becomes sharper. Taken together, this evidence is consistent with domains of PC and SM within individual bilayers rather than macroscopic segregation of phospholipids into different multilamellar aggregates. It can also be seen that the relative X-ray scattering intensity of Peak 2 decreases as the proportion of eggPC decreases. To relate this to the amount of eggPC contributing to the Bragg peaks the scattering intensity from Peak 2 was plotted as a function of the mass of eggPC in the mixture. This is presented in Fig. 9 and gives a straight line passing through the origin. This suggests that eggPC and eggSM are completely phase separated at 50 °C.

4. Discussion

The synchrotron X-ray measurements reported in this study were performed with relatively high angular resolution of the small-angle scattering bands. The Bragg peaks recorded from the lamellar structures have been subjected to detailed analysis to reveal the

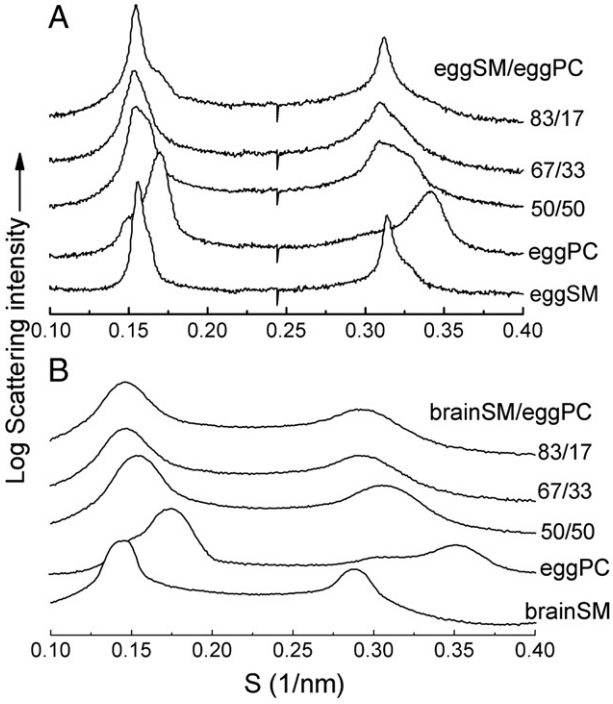

Fig. 8. Logarithm of small-angle X-ray scattering intensity patterns recorded from aqueous dispersions of egg-yolk PC and mixtures of PC with egg-yolk (A) or bovine brain (B) SM at 50 °C.

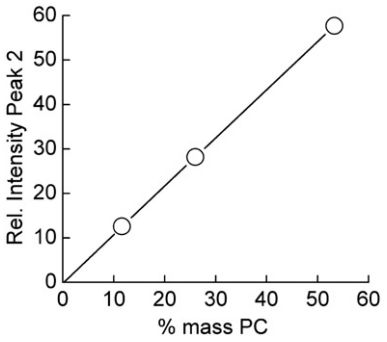

Fig. 9. Plot of relative scattering intensity of Peak 2 (see Table 1) vs % mass of eggPC in binary mixtures with eggSM at 50 °C.

coexistence of lamellar structures in temperature scans between 20 °C and 50 °C. The method of deconvolution of Bragg peaks and calculation of electron density profiles of coexisting bilayer structures to characterize ternary mixtures of diacylglycerophosphatides and cholesterol [10] and ternary mixtures of phosphatidylcholine/sphingomyelin/ceramide and cholesterol [30] have been reported elsewhere. Phase coexistence using this method can be judged from both the SAXS and WAXS regions. In the WAXS region gel and fluid chain packing signatures can be identified in oriented multilayers in mixtures where only a single lamellar structure is observed in the SAXS region [31,32]. Deconvolution of WAXS peaks in powder patterns where the chains are untilted with respect to the bilayer normal can also reveal coexisting packing arrangements of hydrocarbon chains. Thus gel and fluid phase chain packing arrangements can be identified both in the case of coexisting lamellar phases (Fig. 6) and when only a single lamellar structure can be distinguished (Fig. 7). It is noteworthy that coexisting lamellar structures have been observed in binary mixtures of brainSM:eggPC containing 50 mol% or more SM at 23 °C [11] but detection of phase separations from SAXS peaks is known to depend on the extent to which the respective bilayer phases are oriented into stacks.

Peak deconvolution methods applied to powder patterns recorded from dispersions of pure eggPC and eggSM show evidence of fluid–fluid immiscibility of molecular species of eggPC over the temperature range 20 °C–50 °C and gel–gel phase coexistence in eggSM in the temperature range 20 °C–38 °C. The explanation of the reason for fluid–fluid immiscibility in eggPC bilayers is not known but separation of gel phases of eggSM is the result of phase separation of molecular species with hydrocarbon chains able to form an interdigitated structure from those that do not. The relative proportion of interdigitated gel phase (approximately 10%) is consistent with its formation from molecular species comprised of fatty acid chains longer than 18 carbons. There is evidence (Fig. 4) that fluid–fluid phase immiscibility also occurs at temperatures above the gel–fluid phase transition temperature.

Table 1
Structural parameters of mixed aqueous dispersions of eggSM and eggPC at 50 °C.

Mixture* (mole/mole)	Peak 1		Peak 2		Relative intensity
SM:PC	d-spacing	Int/FWHM	d-spacing	Int/FWHM	(% Peak 1)
50:50	6.51	1513	6.24	717	46.7
67:33	6.54	1388	6.35	313	74.0
83:17	6.48	4409	6.36	99	88.4

*Mean values of two independent sets of experiments.

BrainSM shows different patterns of phase behaviour compared to eggSM and this can be attributed to differences in the constituent fatty acids. Whereas the terminal methyl groups of the hydrocarbon chains of most molecular species of eggPC reside along the same central plane of the bilayer the majority of molecular species of brainSM have chain lengths that differ by 4 or more carbon atoms. Molecular dynamics simulation studies [33] and electron density calculations from X-ray diffraction patterns from asymmetric *N*-acyl sphingomyelins [34] indicate partial interdigitation and disorder of the chains in the central plane of the bilayer. This might explain why about 30% of the WAXS profile of brainSM is in a disordered configuration at 20 °C although other forms of $L_{\alpha\beta}$ configurations cannot be excluded [27].

Phase separation in mixed aqueous dispersions of eggSM/DOPC have been reported on the basis of lipid diffusion measurements [35] and occurs at temperatures below the gel to fluid phase transition temperature of eggSM. The existence of domains in mixed monolayers of DOPC with brainSM or eggSM at the air–water interface and supported bilayers has also been reported [36,37] but such experiments are invariably performed at temperatures below the Tm of SM. Even at these temperatures there is evidence from plasmon-waveguide resonance spectroscopy that the phase separated domains are distinct from those of single component bilayers which was interpreted as indicating that each of the separate phases contained small amounts of lipid from the other phase [38]. Phase separation in this mixture at temperatures above Tm has not been reported. Early studies concluded that eggPC and brainSM were completely miscible in all proportions in a liquid–crystal phase at temperatures greater than 44 °C [11]. This conclusion has been confirmed by more recent calorimetric and SAXS/WAXS studies of binary mixtures of eggSM/DOPC which indicated that the two phospholipids were completely miscible in the fluid phase at all molar ratios [39]. Fluorescence probe studies have shown that *N*-stearoyl-SM mixes in a fairly random manner in fluid bilayers of phosphatidylcholine as well as mixtures of phase separated gel and fluid phase phosphatidylcholines whether or not they contain cholesterol [40].

The present X-ray evidence demonstrates that there is extensive fluid–fluid phase immiscibility in mixtures of eggSM and eggPC. Fluid phase immiscibility is consistent with molecular dynamic simulations

of 1:1 mixtures of C18-SM and DOPC which show increasing order of the SM molecules as they form clusters distinct from the more disordered PC molecules [41]. The area/molecule and hydration of SM at the bilayer interface is less than that of PC and, most significantly, SM forms intermolecular H-bonds that result, on molecular dynamics simulations, in a dynamic network characterised by the presence of H-bonded clusters of up to 9 SM molecules [42]. It is noteworthy that the gel to fluid phase transition temperature is shifted down about 5 °C below the Tm observed in pure eggSM and the temperature range between the onset of the transition and its completion is increased. The perturbation of the fluid to gel phase transition could be explained by the presence of numerous, relatively small coexisting fluid domains of eggSM and eggPC above 41 °C. The domains of eggSM are transformed to correspondingly small domains of gel phase on cooling rather than coalescing into more extensive domains of gel and fluid phase.

It is clear from the results presented in Fig. 8 that, unlike eggSM, brainSM is completely miscible with eggPC and this is consistent with previous reports [34]. The forces responsible for immiscibility of the two lipid classes in the fluid phase can be deduced from the differences observed in the hydration of polar groups of C16-SM (similar in *N*-acyl composition to eggSM) and brainSM measured calorimetrically in multibilayer liposomes [43]. According to these findings C16-SM binds only 5.5 molecules of H_2O/lipid compared to 9 molecules of H_2O/molecule of brainSM at comparable levels of hydration. This difference is attributed to greater intermolecular H-bonding between C16-SM molecules because the molecules are aligned coplanar at the lipid–water interface. The lipid–water interface of the brainSM bilayer, by contrast, is irregular because of the mismatch of hydrocarbon chains that are unable to interdigitate in a regular array. Failure to align favourably for formation of intermolecular H-bonds the polar groups becomes hydrated and the cohesion between the molecules is weakened.

It is obvious from the X-ray data that there must be coupling between the two monolayers of the bilayer to give rise to discrete Bragg reflections from coexisting lamellar structures including those assigned to eggSM and eggPC, respectively in mixed dispersions. The nature of such coupling in bilayers of heterogeneous composition is receiving theoretical consideration [44] and domain sizes in the order of 20 nm^2 comprised of 30–40 lipid molecules has been suggested [7].

5. Conclusions

Phase separation of molecular species of PC and SM of biological origin at low temperature into gel and fluid domains is determined by differences in gel to liquid–crystalline phase transition temperature. This, in turn, is determined by van der Waals interactions between aligned hydrocarbon chains given that forces of repulsion are equivalent between the phosphocholine head groups of the two lipid classes. At temperatures above Tm of both phospholipids the factor which determines fluid–fluid immiscibility is the ability to preserve intermolecular H-bonds between the sphingomyelin molecules. If the length of the *N*-acylated fatty acids of the sphingomyelin is longer than the 18 carbons of the sphingosine then interdigitation of the chains in the centre of the bilayer would be required to align the polar groups into favourable orientations for intermolecular H-bonding. Evidence presented here showing complete miscibility of eggPC and brainSM at temperatures above the gel to liquid–crystal phase transition of all the phospholipids indicates that intermolecular H-bond between the sphingomyelin molecules are weakened allowing mixing with eggPC molecules. The ability of cholesterol to create conditions conducive to interdigitation of asymmetric molecular species of sphingomyelin is likely to have a considerable influence on lateral domain formation in bilayers of mixed molecular species of sphingomyelin.

Acknowledgments

The authors thank Anthony Gleeson for assistance in setting up Station 16.1 at the Daresbury SRS and Hiroshi Takahashi for help with data collection at Spring8. Lin Chen, Cedric Tessier and Dominique Rainteau are thanked for assistance in sample preparation and with experiments performed at Daresbury. Funding was provided in part by a grant from the Human Science Frontier Programme (RGP0016/2005C) and grants EC 41008 and 41222 for beamtime at Daresbury and 2006B1043 at Spring8.

Appendix A. Supplementary data

Supplementary data associated with this article can be found, in the online version, at doi:10.1016/j.bbamem.2008.12.011.

References

[1] M. Edidin, The state of lipid rafts: from model membranes to cells, Annu. Rev. Biophys. Biomol. Struct. 32 (2003) 257–283.
[2] K. Simons, E. Ikonen, Functional rafts in cell membranes, Nature 387 (1997) 569–572.
[3] K. Simons, W.L. Vaz, Model systems, lipid rafts, and cell membranes, Annu. Rev. Biophys. Biomol. Struct. 33 (2004) 269–295.
[4] W. Malorni, T. Garofalo, A. Tinari, V. Manganelli, R. Misasi, M. Sorice, Analysing lipid raft dynamics during cell apoptosis, Meth. Enzymol. 442 (2008) 125–140.
[5] J.M. Deeley, T.W. Mitchell, X.J. Wei, J. Korth, J.R. Nealon, S.J. Blanksby, R.J.W. Truscott, Human lens lipids differ markedly from those of commonly used experimental animals, Biochim. Biophys. Acta 1781 (2008) 288–298.
[6] D.J. Cameron, Z.Z. Tong, Z.L. Yang, J. Kaminoh, S. Kaminoh, H.Y. Chen, J.X. Zeng, Y.L. Chen, L. Luo, K. Zhang, Essential role of Elovl4 in very long chain fatty acid synthesis, skin permeability barrier function, and neonatal survival, Int. J. Biol. Sci. 3 (2007) 111–119.
[7] M.D. Collins, Interleaflet coupling mechanisms in bilayers of lipids and cholesterol, Biophysical. J. 94 (2008) L32–L34.
[8] T.J. McIntosh, S.A. Simon, D. Needham, C.H. Huang, Structure and cohesive properties of sphingomyelin cholesterol bilayers, Biochemistry 31 (1992) 2012–2020.
[9] H.J. Risselada, S.J. Marrink, The molecular face of lipid rafts in model membranes, Proc. Natl. Acad. Sci. (USA) 105 (2008) 17367–17372.
[10] L. Chen, Z. Yu, P.J. Quinn, The partition of cholesterol between ordered and fluid bilayers of phosphatidylcholine: a synchrotron X-ray diffraction study, Biochim. Biophys. Acta 1768 (2007) 2873–2881.
[11] S.H. Untracht, G.G. Shipley, Molecular interactions between lecithin and sphingomyelin. Temperature- and composition-dependent phase separation, J. Biol. Chem. 252 (1977) 4449–4457.
[12] A. Pokorny, L.E. Yandek, A.I. Elegbede, A. Hinderliter, P.F.F. Almeida, Temperature and composition dependence of the interaction of δ-Lysin with ternary mixtures of sphingomyelin/cholesterol/POPC, Biophys. J. 91 (2006) 2184–2187.
[13] W.I. Calhoun, G.G. Shipley, Sphingomyelin-lecithin bilayers and their interaction with cholesterol, Biochemistry 18 (1979) 1712–1722.
[14] P.R. Maulik, G.G. Shipley, Interactions of *N*-stearoyl sphingomyelin with cholesterol and dipalmitoylphosphatidylcholine in bilayer membranes, Biophys. J. 70 (1996) 2256–2265.
[15] L.K. Bar, Y. Barenholz, T.E. Thompson, Effect of sphingomyelin composition on the phase structure of phosphatidylcholine-sphingomyelin bilayers, Biochemistry 36 (1997) 2507–2516.
[16] B. Terova, J.P. Slotte, T.K.M. Nyholm, Miscibility of acyl-chain defined phosphatidylcholines with *N*-palmitoyl sphingomyelin in bilayer membranes, Biochim. Biophys. Acta 1667 (2004) 182–189.
[17] T. Nyholm, M. Nylund, A. Soderholm, J.P. Slotte, Properties of palmitoyl phosphatidylcholine, sphingomyelin, and dihydrosphingomyelin bilayer membranes as reported by different fluorescent reporter molecules, Biophys. J. 84 (2003) 987–997.
[18] J. Villalain, A. Ortiz, J.C. Gomez-Fernandez, Molecular interactions between sphingomyelin and phosphatidylcholine in phospholipid vesicles, Biochim. Biophys. Acta 941 (1988) 55–62.
[19] M.P. Veiga, J.L.R. Arrondo, F.M. Goni, A. Alonso, D. Marsh, Interaction of cholesterol with sphingomyelin in mixed membranes containing phosphatidylcholine, studied by spin-label ESR and IR spectroscopies. A possible stabilization of gel-phase sphingomyelin domains by cholesterol, Biochemistry 40 (2001) 2614–2622.
[20] A. Filippov, G. Oradd, G. Lindblom, Lipid lateral diffusion in ordered and disordered phases in raft mixtures, Biophys. J. 86 (2004) 891–896.
[21] E.J. Addink, J. Beintema, Polymorphism of crystalline polypropylene, Polymer 2 (1961) 185–187.
[22] C. Boulin, R. Kempf, M.H. Koch, S.M. McLauchlin, Data appraisal, evaluation and display for synchrotron radiation experiments: hardware and software, Nuc. Instr. Meth. Physical Res. A249 (1986) 399–407.
[23] R. Zhang, R.M. Suter, J.F. Nagle, Theory of the structure factor of lipid bilayers, Phys. Rev. E. 50 (1994) 5047–5060.

[24] T. Yao, H. Jinno, Polarization factor for the X-ray-powder diffraction method with a single-crystal monochromator, Acta Crys. A. 38 (1982) 287–288.
[25] G. Pabst, R. Koschuch, B. Pozo-Navas, M. Rappolt, K. Lohner, P. Laggner, Structural analysis of weakly ordered membrane stacks, J. Appl. Cryst. 36 (2003) 1378–1388.
[26] E. Sackmann, in: R. Lipowsky, E. Sackmann (Eds.), Structure and dynamics of membranes, Amsterdam, North Holland, 1995, pp. 213–304.
[27] J.L. Ranck, L. Mateu, D.M. Sadler, A. Tardieu, T. Gulik-Krzywicki, V. Luzzati, Order–disorder conformational transitions of the hydrocarbon chains of lipids, J. Mol. Biol. 85 (1974) 249–277.
[28] T.J. McIntosh, Effect of cholesterol on structure of phosphatidylcholine bilayers, Biochim. Biophys. Acta 513 (1978) 43–58.
[29] C. Chachaty, D. Rainteau, C. Tessier, P.J. Quinn, C. Wolf, Building up of the liquid-ordered phase formed by sphingomyelin and cholesterol, Biophys. J. 88 (2005) 4032–4044.
[30] G. Staneva, C. Chachaty, C. Wolf, K. Koumanov, P.J. Quinn, The role of sphingomyelin in regulating phase coexistence in complex lipid model membranes: competition between ceramide and cholesterol, Biochim. Biophys. Acta (2008), doi:10.1016/j.bbamem.2008.07.025.
[31] T.T. Mills, S. Tristram-Nagle, F.H. Heberle, N.F. Morales, J. Zhao, J. Wu, G.E.S. Toombes, J.F. Nagle, G.W. Feigenson, Liquid–liquid domains in bilayers detected by wide angle X-ray scattering. Biophys J. doi:10.1529/biophysj.107.127910.
[32] T.T. Mills, G.E.S. Toombes, S. Tristram-Nagle, D-M. Smilgies, G.W. Feigenson, J.F. Nagle. Order parameters and areas in fluid-phase oriented lipid membranes using wide angle X-ray scattering. Biophys J. doi:10.1529/biophysj.107.127845.
[33] P.S. Niemela, M.T. Hyvonen, I. Vattulainen, Influence of chain length and unsaturation on sphingomyelin bilayers, Biophys. J. 90 (2006) 851–863.
[34] P.R. Maulik, D. Atkinson, G.G. Shipley, X-ray scattering of vesicles of *N*-acyl sphingomyelins: determination of bilayer thickness, Biophys. J. 50 (1986) 1071–1077.
[35] G. Lindblom, G. Oradd, A. Filippov, Lipid lateral diffusion in bilayers with phosphatidylcholine, sphingomyelin and cholesterol—an NMR study of dynamics and lateral phase separation, Chem. Phys. Lipids 141 (2006) 179–184.
[36] J.C. Lawrence, D.E. Saslowsky, J.M. Edwardson, R.M. Henderson, Real-time analysis of the effects of cholesterol on lipid raft behavior using atomic force microscopy, Biophys. J. 84 (2003) 1827–1832.
[37] E. Prenner, G. Honsek, D. Honig, D. Mobius, K. Lohner, Imaging of the domain organization in sphingomyelin and phosphatidylcholine monolayers, Chem. Phys. Lipids 145 (2007) 106–118.
[38] Z. Salamon, S. Devanathan, I.D. Alves, G. Tollin, Plasmon-waveguide resonance studies of lateral segregation of lipids and proteins into microdomains (rafts) in solid-supported bilayers, J. Biol. Chem. 280 (2005) 11175–11184.
[39] G. Degovics, A. Latal, E. Prenner, M. Kriechbaum, K. Lohner, Structure and thermotropic behaviour of mixed choline phospholipid model membranes, J. Appl. Cryst. 30 (1997) 776–780.
[40] T.Y. Wang, J.R. Silvius, Sphingolipid partitioning into ordered domains in cholesterol-free and cholesterol-containing lipid bilayers, Biophys. J. 84 (2003) 367–378.
[41] S.A. Pandit, E. Jakobsson, H.L. Scott, Simulation of the early stages of nano-domain formation in mixed bilayers of sphingomyelin, cholesterol, and dioleylphosphatidylcholine, Biophys. J. 87 (2004) 3312–3322.
[42] E. Mombelli, R. Morris, W. Taylor, F. Fraternali, Hydrogen-bonding propensities of sphingomyelin in solution and in a bilayer assembly: a molecular dynamics study, Biophys. J. 84 (2003) 1507–1517.
[43] M. Kodama, M. Abe, Y. Kawasaki, S. Ohira, H. Nozaki, C. Katagiri, K. Inoue, H. Takahashi, Estimation of interlamellar water molecules in sphingomyelin bilayer systems studied by DSC and X-ray diffraction, Thermochim. Acta 416 (2004) 105–111.
[44] A.J. Wagner, S. Loew, S. May, Influense of monolayer–monolayer coupling on the phase behavior of a fluid lipid bilayer, Biophys. J. 93 (2008) 4268–4277.